Bent-Beam Electrothermal Actuators—Part I: Single Beam and Cascaded Devices

Long Que, *Member, IEEE*, Jae-Sung Park, and Yogesh B. Gianchandani, *Member, IEEE*

***Abstract*—This paper describes electrothermal microactuators that generate rectilinear displacements and forces by leveraging deformations caused by localized thermal stresses. In one manifestation, an electric current is passed through a V-shaped beam anchored at both ends, and thermal expansion caused by joule heating pushes the apex outward. Analytical and finite element models of device performance are presented along with measured results of devices fabricated using electroplated Ni and p^{++} Si as structural materials. A maskless process extension for incorporating thermal and electrical isolation is described. Nickel devices with 410-μm-long, 6-μm-wide, and 3-μm-thick beams demonstrate 10 μm static displacements at 79 mW input power; silicon devices with 800-μm-long, 13.9-μm-wide, and 3.7-μm-thick beams demonstrate 5 μm displacement at 180 mW input power. Cascaded silicon devices using three beams of similar dimensions offer comparable displacement with 50–60% savings in power consumption. The peak output forces generated are estimated to be in the range from 1 to 10 mN for the single beam devices and from 0.1 to 1 mN for the cascaded devices. Measured bandwidths are $\approx$ 700 Hz for both. The typical drive voltages used are $\leq$ 12 V, permitting the use of standard electronic interfaces that are generally inadequate for electrostatic actuators. [592]**

***Index Terms*—Micromachining, micromotors, positioners, thermal actuators.**

I. Introduction

A MAJORITY of actuators that have been developed in the past using micromachining technology utilize transduction mechanisms that are not available in silicon. These actuators typically require the incorporation of magnetic or piezoelectric materials [1], [2], shape memory alloys [3], or even encapsulated fluids [4]. In some applications the use of these materials is prevented by processing constraints or other considerations, and the options are limited to silicon-based actuators, which generally use electrostatic or electrothermal transduction.

The forces generated by both parallel plate and comb-driven electrostatic actuators [5] rarely exceed 10 μN in surface micromachined devices, and are often lower than 1 μN [6]. Higher forces have been demonstrated with scratch drive actuators [7]–[9] but the displacement from each thrust is < 100 nm, and must be accumulated over multiple cycles. With other electrostatic mechanisms the displacements rarely exceed 100 μm in resonant operation and 10 μm in nonresonant operation, unless gear-trains, inchworms, or other stepping mechanisms are used to accumulate the displacement. Although electrostatic actuators have many advantages such as low temperature coefficients and essentially zero dc power consumption, they require high voltages ($\geq$ 30 V) that can be incompatible not only with microelectronic power supplies, but with silicon substrates and integrated circuits as well. The incompatibility arises from concerns of dielectric oxide and junction breakdown, and the need to expand layout to accommodate the larger depletion widths associated with elevated voltages. Moreover, with high electric fields on the device surface, the risk of arcing can make the device sensitive to environmental variables such as ambient pressure and humidity [10].

Past approaches to electrothermal actuation rely on the bending moment created by heating two adjacent materials with different expansion coefficients. Although relatively large forces and substantial displacements can be generated, some important compromises are involved. For example, the motion is typically associated with the bending of a cantilever, and is not rectilinear. Moreover, bimorphs are generally made for out-of-plane actuation [11]. Although out-of-plane actuators can be used for in-plane displacements [12], [13], the in-plane forces are typically $< 10\,\mu$N. Arrayed out-of-plane actuators have been used as conveyors and positioners [14]–[16]. Planar actuation (parallel to the device substrate) is particularly difficult to achieve since laying the bimorph materials side-by-side complicates the fabrication sequence, and does not necessarily produce a large rectilinear displacement [17]. However, the requirement for disparate materials may be circumvented by using a structure that has two adjacent arms of different widths, resulting in a pseudobimorph [18], [19]. Such devices require only one structural material even though they operate very much like bimorphs. They are able to accomplish planar motion (parallel to the substrate), with displacements for the polysilicon devices exceeding 20 μm [20]. The locus of motion is an arc, and the forces reported are typically below 20 μN. Recently, certain synthesized designs have also been reported [21], [22]. Although most of the past efforts at electrothermal actuation have used polysilicon or electroplated metals as the structural material, shape memory alloy has also been utilized [23]. This material can provide very large displacements and forces, but poses a significant challenge in process integration. In general, electrothermal actuators consume more power

Manuscript received June 27, 2000. The work of Y. B. Gianchandani was supported in part by a National Science Foundation Career Award (ECS-9985422). Subject Editor E. Obermeier.

L. Que was with the Department of Electrical and Computer Engineering, University of Wisconsin, Madison, WI 53706 USA. He is now with OpticNet, Inc., Campbell, CA 95008 USA.

J.-S. Park is with the Department of Mechanical Engineering, University of Wisconsin, Madison, WI 53607 USA.

Y. B. Gianchandani is with the Department of Electrical and Computer Engineering, University of Wisconsin, Madison, WI 53607 USA (e-mail: yogesh@engr.wisc.edu).

Publisher Item Identifier S 1057-7157(01)04263-9.

1057–7157/01$10.00 ©2001 IEEE

than electrostatic ones, but they provide higher forces and can be driven with lower voltages, allowing standard interface electronics to be used.

This article describes in-plane electrothermal actuators based on bent-beam suspensions that have been used very successfully for strain sensing [24].[1] When an electric current is passed through a V-shaped beam anchored at its two ends, thermal expansion caused by joule heating pushes the apex outward (Fig. 1) [26], [27]. *Bent-beam actuators are fundamentally different from bimorph actuators in that they produce rectilinear displacements and do not use structural segments with differing thermal expansions*. (Similar parallelogram shapes have also been used to amplify electrostatically generated displacements [25].) Compared to other electrothermal devices that provide in-plane motion, bent-beam actuators offer an attractive compromise of displacement, force, scalability and simplicity in design. They can be fabricated with any material that is electrically conductive and has the mechanical strength to serve as an actuator. Both p^{++} Si and electroplated Ni are explored as structural materials in this effort. Section II describes analytical and finite element modeling (FEM) of these microactuators; Section III describes the fabrication process and the experimental results, including displacement and bandwidth measurements and force estimates; and Section IV provides the conclusions. An accompanying article that follows this one describes the use of bent-beam actuators in rotary and rectilinear microengines [28].

II. Device Structure and Modeling

The simplest manifestation of bent-beam electro-thermal actuators is a V-shaped beam operated as shown in Fig. 1. The displacement of the apex is a function of the beam dimensions and slope. It is reduced in almost linear proportion to the magnitude of the external loading force, f(Fig. 2). The maximum displacement, $d_{\max}$, obtained in the absence of f, can be calculated analytically from the beam bending equation with a correction term for the beam compression [24]:

$$\begin{aligned} d_{\max} &= 2\frac{\tan\theta_1}{k}\tan\frac{kL_1}{4} - \frac{L_1}{2}\tan\theta_1; \\ \Delta T &= \frac{1}{\alpha\cdot L_1}\left(\Delta L' + \frac{FL_1}{EWH}\right); \quad k=\sqrt{\frac{F}{EI}} \\ L' &= \frac{(\tan\theta_1)^2}{4k}\left[2G + kL_1 + kL_1G^2 + \sin kL_1 \right. \\ &\qquad \left. - 2G\cos kL_1 - G^2\sin kL_1\right] \end{aligned} \tag{1}$$

where

G	$\tan(kL_1/4)$;
H	$\tanh(kL_1/4)$;
E	Young's modulus;
α	expansion coefficient;
H	beam thickness;
W	beam width;
I	moment of inertia of the beam;
L_1	length defined in Fig. 2;
θ_1	bending angle defined in Fig. 2;
F	reaction force along the x-axis at the anchors;
ΔT	temperature change;
$\Delta L'$	change in L' due to F;

[1]Portions of this paper have appeared in conference abstract form [26].

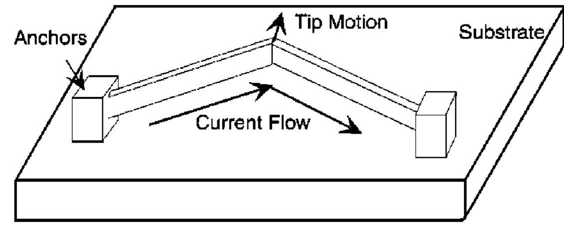

Fig. 1. Structure and operation of a basic single bent beam actuator. Current passing through a suspended beam causes joule heating, resulting in a displacement of the apex which is amplified by the bending angle of the beam.

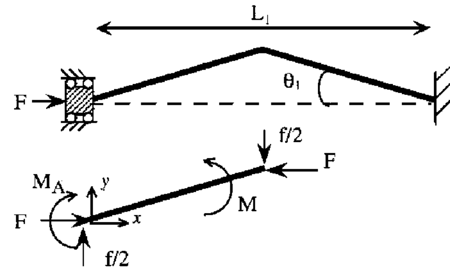

Fig. 2. Forces acting on a bent-beam thermal actuator. The external loading force is labeled f.

It is accurate to within 5% of finite element analysis (FEA). The comparison to FEA was performed for 500–2000 μm length, 4–5 μm width and thickness, and 0.025–0.2 radian bending angle.

The maximum loading force that can be sustained at the apex, $f_{\max}$, is defined as that at which the displacement of the apex is forced back to zero. It can be calculated analytically to within about 10% of the FEA value by using a formula derived by the complementary energy method:

$$f_{\max} = d_{\max};\, K_y; K_y = \frac{4\sin^2(\theta_1')AE}{L_1} \tag{2}$$

where $A = W_1H$ is the cross-sectional area of the beam, and θ_1' is the effective bending angle, which may differ from the designed angle as a result of the displacement of the apex, particularly in long beams with a shallow bending angle. Note that the load lines of Fig. 2 can exhibit some nonlinearity near $f_{\max}$. Equation (2) accommodates beam compression, but ignores bending because strain energy for this is relatively small. The consistency of this formula with FEA was validated for the same dimensional parameters mentioned above, but over a reduced range of 0.05–0.2 rad. for θ_1.

Clearly, device performance can be altered by changing the geometry of the beam. In general, the peak displacement of a beam at a given temperature can be increased by making the beam longer or by reducing the bending angle. A higher peak force can be obtained by the opposite changes. The thickness and width of the beam affect the output force in direct proportion. In addition to changes in the beam geometry, higher forces can be generated by placing bent-beam actuators in parallel, and larger displacements can be generated by cascading the actuators. For cascaded actuators, if two primary base units are driven

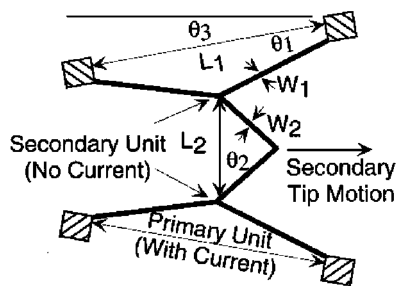

Fig. 3. Cascaded bent-beams can be used to further amplify motion. If current is confined to the two primary units, the secondary unit serves exclusively as a motion amplifier. The diagram shows the notation used for various dimensions. Beam thickness is denoted by H.

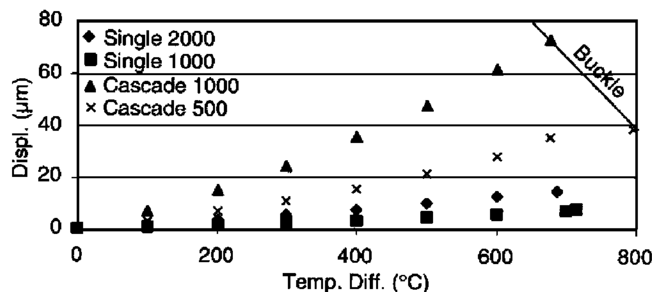

Fig. 4. Nonlinear FEA of Si actuators. Single: $H = 4.5$ μm, $W_1 = 6$ μm, $\theta_1 = 0.2$ rad, $L = 1000/2000$ μm. Cascaded: $H = 4.5$ μm, $W_1 = 6$ μm, $W_2 = 4$ μm, $\theta_1 = 0.1$ rad, $\theta_2 = 0.2$ rad, $L_1 = L_2 = 500/1000$ μm, secondary unit was unheated.

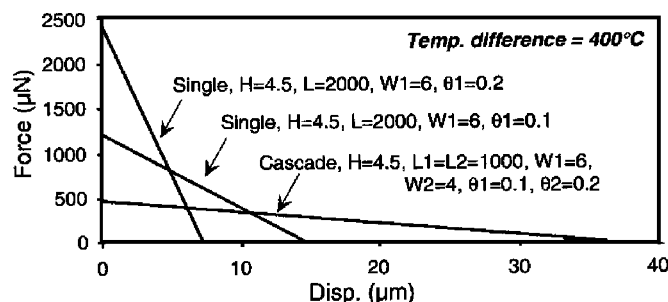

Fig. 5. FEA load lines of Si actuators at 400 °C. In the cascaded device, the secondary unit was unheated.

by the same voltage source, the current through the secondary unit will be nominally zero (Fig. 3). Cascaded devices have significantly larger displacement than simple beams even when the secondary unit is not heated. However, a caveat associated with all large structures, including cascaded arrangements, is that the critical force for vertical (out-of-plane) buckling is reduced. To compensate, the operating temperatures for these devices must be reduced or the thickness of the devices must be increased.

In (1), it was assumed that the expansion coefficient of the structural material is not a function of temperature. Although this makes the analytical solution more tractable, it underestimates the displacement by about 30% for Si devices. The expansion coefficient of Si increases from about 2.5 ppm/K at room temperature to 4 ppm/K at 500 °C [29]. Using an expression for the expansion coefficient that provides a linear fit through these points, displacement and force curves were obtained by nonlinear FEA using ANSYS. It was assumed that the substrate does not expand since the net input power is very low. It was also assumed that the actuator has a uniform temperature change along its entire length. This basically means that the primary heat loss from a segment of the beam is to the surrounding rather than to the anchor. Displacements obtained for devices of various dimensions are shown in Fig. 4. Single beam devices of 1–2 mm length can provide about 10 μm of displacement at an operating temperature of 600 °C, whereas cascaded arrangements can provide more than 30 μm displacement under similar conditions. The FEA also shows that there is a linear tradeoff between the loading force and the displacement (Fig. 5), which holds for single beam as well as cascaded devices in the range of dimensional parameters tested. Peak forces for the noted examples were in the range of a few millinewtons. These values increase with beam width. It should be noted that the dimensions used for these examples are purely illustrative, and have not been optimized for any particular application.

A. Temperature, Power, and Choice of Materials

Polysilicon, p^{++} Si, and electroplated Ni are commonly used structural materials for MEMS, and are good candidates for electro-thermal actuators. The expansion coefficient of electroplated Ni is upto 12–16 ppm/K, which is about four times higher than that of Si. Although this can result in larger displacement for Ni devices, the position of the apex may also change with the ambient temperature because of its expansion mismatch with the substrate, which is typically Si or a type of glass that is expansion matched to Si. While polysilicon devices are expected to operate up to about 600 °C (above which *in situ* annealing can be a threat), and p^{++} Si structures may accommodate even higher temperatures, the upper limit for Ni structures is about 350 °C, beyond which an irreversible darkening of the structure is observed to occur (possibly due to oxidation), along with degradation of the actuation stroke.

Since the thermal isolation of most microstructures with respect to the substrate and the ambient is 1000–10 000 K/W, maintaining a temperature of 600 °C requires only 60–600 mW of power [31]. Moreover, the actuation voltages are typically ≤ 12 V, permitting the use of standard electronic interfaces that are generally inadequate for many electrostatic actuators.

III. Fabrication and Test

Electrothermal actuators were fabricated with electroplated Ni and with single crystal silicon. The Ni devices were fabricated on a Si substrate with a 2-μm-thick plasma enhanced chemical wafer deposited (PECVD) oxide isolation layer capped by a 5-kÅ-thick PECVD nitride layer. A 2-μm-thick Ti sacrificial layer was then deposited, followed by a seed layer. The structural Ni was plated into a photoresist mold using a sulfamate solution. Plating was performed at 50–55 °C with current densities of 5–10 mA/cm^2. Following this, the mold was stripped and the seed and sacrificial layers were etched to release the devices. In a variation of this process the Ni structures were then selectively plated with ≈500 Å Au by immersing for 10 min in an electroless plating solution (Alfa Aesar #42 307) at 60 °C. The Au coating appears to elevate the operating limit from $\approx 350\,^{\circ}$C to $\approx 450\,^{\circ}$C. This increases the peak displacements achievable with Ni devices.

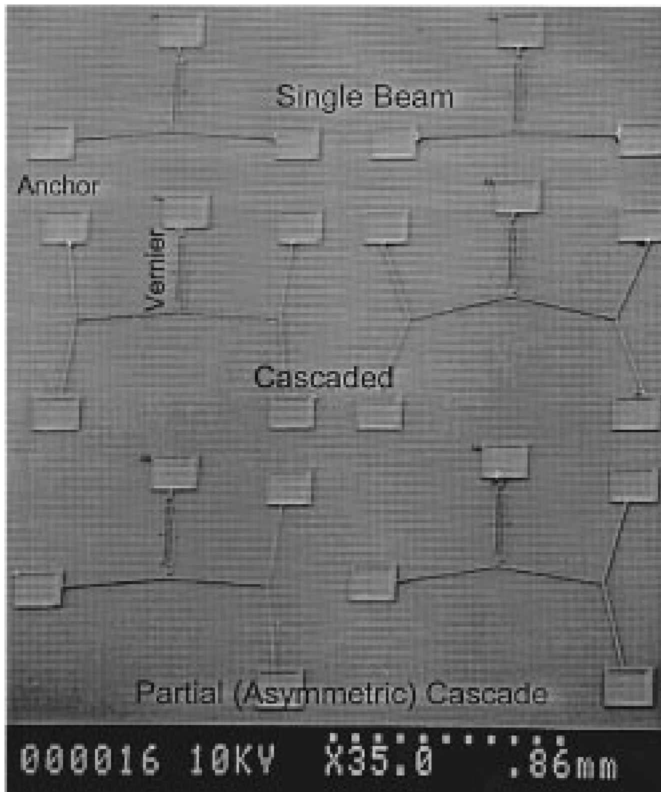

Fig. 6. An array of $3.7~\mu$m thick p^{++} Si actuators, including single beam (top row), symmetrical single cascade (center row), and asymmetrical single cascade (bottom row), at various bending angles. All devices have integrated verniers to permit precise measurements of deflection.

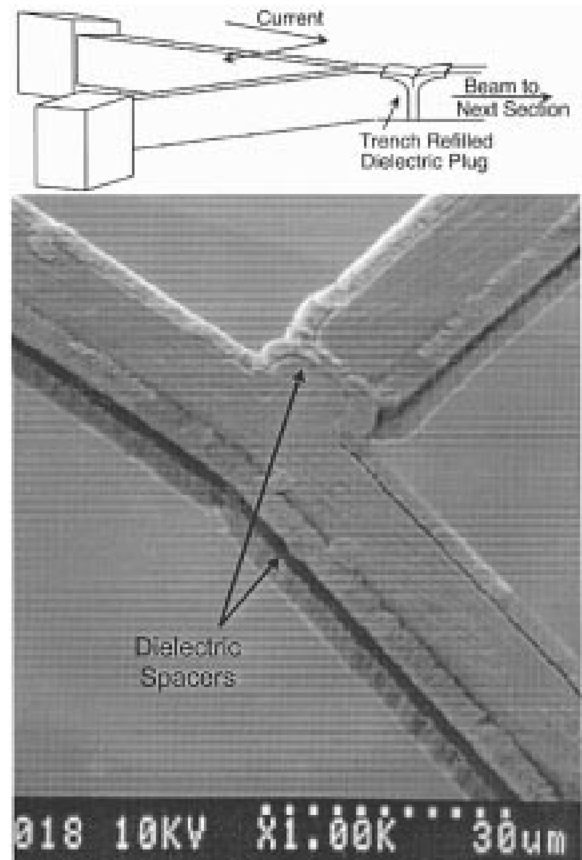

Fig. 7. Dielectric sidewall spacers added without additional lithography steps can be used optionally to isolate current and heat in localized portions of the devices (see arrows).

The Si devices were fabricated by the dissolved wafer process [30]. The sequence involved first recessing an Si wafer everywhere except at the device anchors, then performing an unmasked boron diffusion to define the thickness of the microstructures. This was followed by a vertical dry etch through the boron diffused layer to define the shape of the microstructures. The silicon wafer was then anodically bonded to a glass wafer and the undoped Si dissolved in EDP, leaving the microstructures attached to the glass substrate.

Some of the fabricated samples were coated with self-assembled monolayers after the sacrificial layer etch in order to circumvent stiction-related problems. A set of fabricated p^{++} Si actuators is shown in Fig. 6. The devices were equipped with integrated vernier scales to measure displacement. The resolution of the verniers was $0.2–0.5~\mu$m, depending upon the design.

A. Electrical and Thermal Isolation

A potential drawback of thermal actuators is the ability to confine the current and heat flow for applications that are sensitive to these parameters. However, this can be addressed by a maskless extension to the fabrication process that provides dielectric sidewall spacers. This requires a minor modification in the device layout to provide cuts in the beams at the desired isolation points. A blanket deposition of dielectric such as PECVD or LPCVD nitride or oxide followed by a maskless anisotropic dry etch forms dielectric sidewalls for the device that also refill the cuts (Fig. 7). A number of cuts can be located in series along a beam to increase thermal isolation as desired. This approach extension adds minimal complexity, and can easily be integrated into a standard MEMS or IC process.

B. Measurements of Displacement, Force, Speed, Reliability

Fig. 8 shows the measured displacement response for single beam and cascaded p^{++} Si actuators. The single beam device was 800-μm long, 13.9-μm wide, 3.7-μm thick, and had a bending angle of 0.2 rad. With no external loading it generated a static displacement ($d_{\max}$) of 5 μm at $\approx$ 180 mW input power, which required a 12-V bias. The loading force $f_{\max}$, necessary to reduce the displacement to zero, was calculated from (2) for the specific dimensions of this device, and is marked on the right vertical axis of Fig. 8(a). The value of Young's modulus used in these calculations was 180 GPa. Under these conditions, a $d_{\max}$ of 5 μm corresponds to an $f_{\max}$ of 8.3 mN. The cascaded actuator had three identical beam elements that were similar to the single beam actuator except that the bending angle was 0.1 rad. This device generated 3 μm displacement at 40 mW input power, which required a 2.9-V bias. Both primary units were driven by the same power supply. For the cascaded actuators, the force $f_{\max}$ corresponding to each $d_{\max}$ was determined by FEA, yielding 132 μN for 3 μm using the specific dimensions of this device. Both plots in Fig. 8 show an approximately linear relationship between the maximum displacement and the input power, suggesting that conductive heat loss dominates in the tested region of

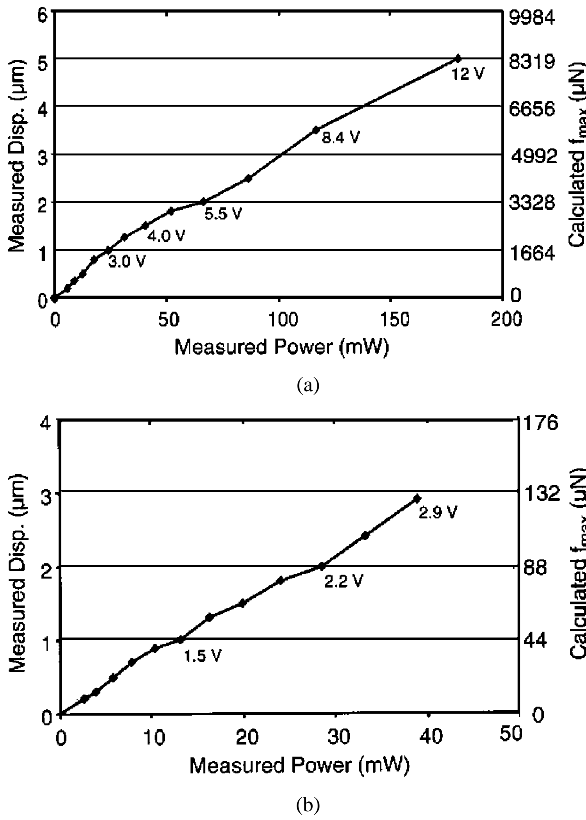

Fig. 8. Measured $d_{\max}$ and the corresponding calculated $f_{\max}$ versus input power. Actuation voltages are indicated at selected points. (a) A p^{++} Si single beam actuator. (b) A cascaded p^{++} Si actuator.

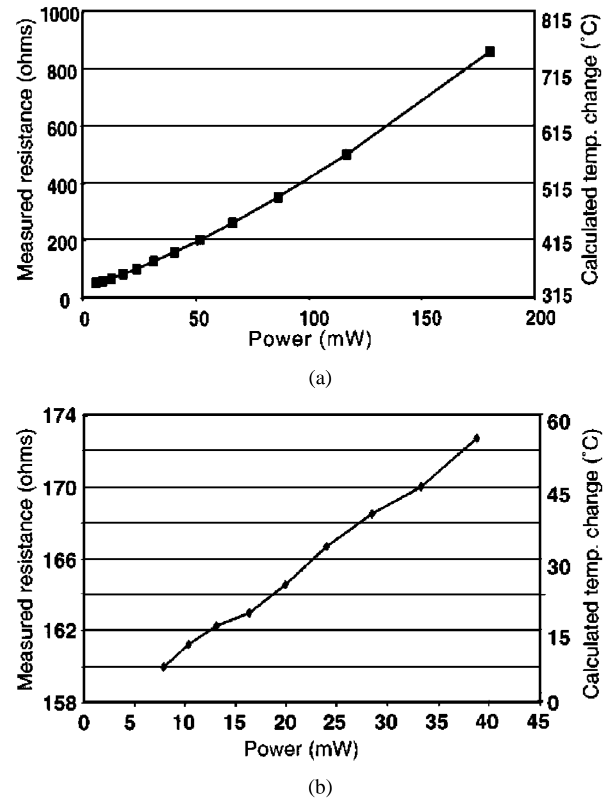

Fig. 9. Resistance variation versus input power for Fig. 8(a) and (b). The *average* temperature change corresponding to each resistance value is shown on the right vertical axis in each case.

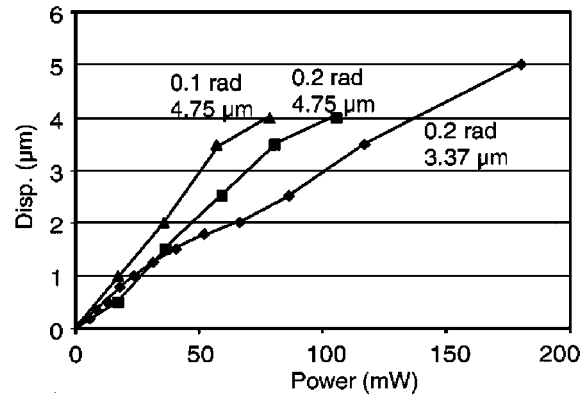

Fig. 10. Measured $d_{\max}$ of single beam p^{++} Si actuators as a function of input power. $L_1 = 800\ \mu$m, $W_1 = 13.9\ \mu$m, H and θ_1 as indicated.

operation. The minor variations from linearity are probably due to the vernier resolution limit.

The average increase in temperature in a single beam actuator or in the primary units of a cascaded actuator can be estimated from the change in resistance as the input power is increased. Fig. 9(a) and (b) plots the resistance and the corresponding increase in average temperature for the devices of Fig. 8(a) and (b), respectively. A value of 1818 ppm/K was used as the temperature coefficient of resistance (TCR) of p^{++} Si [31]. Piezoresistance effects were ignored because the devices were tested without external loading, and the thermal stress is almost entirely relieved by the displacement. Even for cases in which residual stress may exist in the deformed devices, piezoresistance effects can account for only about 15% of the net resistance change because the TCR is relatively large.

Fig. 10 compares displacement measurements obtained from three p^{++} Si single beam actuators which differed in bending angle. All three devices were 800 μm long, 13.9 μm wide, and 3.37 μm or 4.75 μm thick, as indicated in the figure. As predicted by theory, the 0.1 rad. bending angles result in larger displacements than 0.2 rad angles. However, they create higher compressive forces that may lead to lower operating lifetimes. (This aspect of performance is under investigation, and will be reported separately.) In addition, the buckling temperature reduces as the bending angles are decreased.

Fig. 11 compares the performance of several cascaded p^{++} Si actuators. In each case the beam segments are 800 μm long, 13.9 μm wide, and 3.37 μm or 4.75 μm thick. Bending angles vary between devices, as indicated on the figure, although all three segments of each actuator have the same bending angle. Shallow bending angles are associated with higher displacements in these devices as well.

Fig. 12 shows the measured static displacement as a function of input current for an electroplated Ni single beam device with 410 μm length, 6 μm width, 3 μm thickness, and 0.05 rad bending angle. The relationship appears quadratic, as expected, since the input power to the actuator is related to the square root of the device current. The figure also shows that relatively high currents may be needed for actuation when the actuator resistance is very low, as in this case. At 210 mA input current the

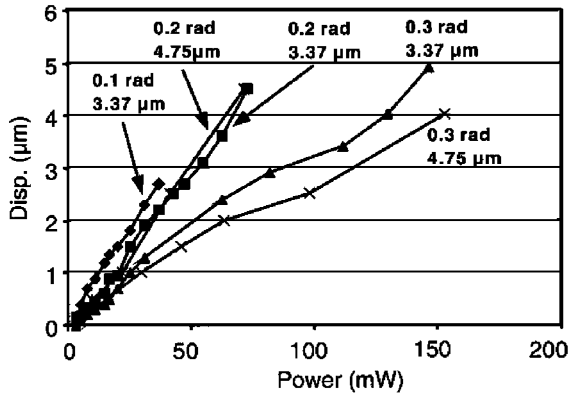

Fig. 11. Measured $d_{\max}$ of cascaded p^{++} Si actuators as a function of input power. $L_1 = L_2 = 800$ μm, $W_1 = W_2 = 13.9$ μm, H and $\theta_1 = \theta_2$ are as indicated.

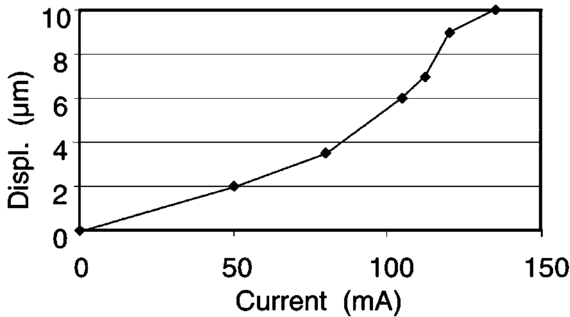

Fig. 12. Measured displacement of a plated Ni actuator with $L_1 = 410$ μm, $W_1 = 6$ μm, $H = 3$ μm, and $\theta_1 = 0.05$ rad. The resistance of the device was ≈ 5.5 Ω at 120 mA, corresponding to 79.2 mW input power.

resistance of this device was 5.5 Ω, corresponding to 79.2 mW of input power.

Thermal actuators are generally slower than electrostatic ones because the thermal time constants involved are longer than the electrical and mechanical time constants for many microstructures. However, preliminary tests for both simple and cascaded devices indicate that nonresonant actuation frequencies in excess of 1 kHz are reasonable (Fig. 13). The measured -3 db bandwidth for both devices was ≈700 Hz. This relatively high bandwidth exists because of the very small thermal mass of these structures.

For the devices used in this effort, the primary heat loss is by conduction to the substrate, which occurs through the air gap underneath the beam and through the anchors. It is worth noting that while testing, no cross-talk was ever observed between devices—even those in close proximity to each other. This implies that the heating is well isolated, and that standard microsensor packages can be used. Additionally, if the heat (and current) are further confined to selected beams by the technique illustrated in Fig. 7, short thermal time constants can be maintained even for larger and more complex mechanisms.

Preliminary tests were conducted to assess the reliability of p^{++} Si single beam actuators. A device similar to that used for Fig. 8(a) was exercised with a 6-V, 300-Hz square wave for a total of six million cycles. There was no degradation in the amplitude of the motion to the extent that could be determined by the integrated vernier. However, it is reasonable to expect that

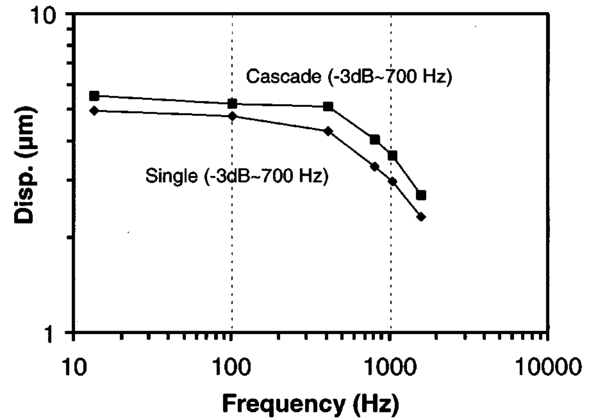

Fig. 13. Measured frequency response of p^{++} Si thermal actuators with $L = 800$ μm, $W = 13.9$ μm, $H = 3.7$ μm, and $\theta = 0.2$ rad. The drive signals were 10 (4.1) V square waves for the single (cascaded) device.

device lifetime is related to drive amplitude. Additional studies are being conducted to determine the operation limits, which will be reported separately [32].

IV. Conclusion

This effort has examined simple and cascaded arrangements of bent beam thermal actuators. The devices were modeled both analytically and by FEA, showing that the former approach is suitable for a wide range of temperatures, and also showing that the device response in both peak force and displacement is linearly related to temperature (and thus input power). A number of different devices were fabricated using p^{++} Si and electroplated Ni as the structural materials. Measurements verified that displacements of 10 μm could be achieved by single beam (Ni) devices with a power dissipation of 80 mW, and output forces > 8 mN could be achieved (in p^{++} Si devices) with input power < 250 mW. It was also demonstrated that cascaded devices offered an improvement of about 2–4× in displacement. The Ni devices offer larger displacements than the Si devices at equal temperatures because of the higher expansion coefficient of the former material. However, the peak operating temperature of the Si devices is higher. The Ni devices require current in the 100 mA range and voltage in the 2 V range, because they typically have resistance < 10 Ω. In contrast, the Si devices require current in the range of 10 mA range and voltage typically ≤ 12 V, which are easier to supply through standard integrated circuits. The operational frequency range of both single beam and cascaded p^{++} Si devices was shown to exceed 1 kHz. With the electrical and thermal isolation scheme that was presented, it may be possible to sustain these bandwidths for larger structures as well.

In summary, with the displacements, forces, operating frequencies, power consumption, and actuation voltages demonstrated, bent-beam actuators may offer suitable compromises for drive options in several microelectromechanical applications.

Acknowledgment

The authors gratefully acknowledge M.-H. Li for helping with the device measurements, Prof. J. Hetrick for discussions,

and the staff of the Wisconsin Center for Applied Microelectronics for technical support.

REFERENCES

[1] H. Guckel, K. Fisher, and E. Stiers, "Closed loop controlled, large throw, magnetic linear microactuator with 1000 μm structural height," in *Proc. IEEE International Workshop on Micro Electro Mechanical Systems (MEMS'98)*, Heidelberg, Germany, Jan. 1998, pp. 414–418.

[2] A. M. Flynn, L. S. Tavrow, S. F. Bart, R. A. Brooks, D. J. Ehrlich, K. R. Udayakumar, and L. E. Cross, "Piezoelectric Micromotors," *J. Microelectromech. Syst.*, vol. 1, pp. 44–52, Mar. 1992.

[3] P. W. Barth, "Silicon microvalves for gas flow control," in *Proc. IEEE Int. Conference on Solid-State Sensors and Actuators (Transducers '95)*, vol. 2, Stockholm, Sweden, June 1995, pp. 276–280.

[4] M. J. Zdeblick, R. Anderson, J. Jankowski, B. Klein-Schoder, L. Christel, R. Miles, and W. Weber, "Thermopneumatically actuated microvalves and integrated electro-fluidic circuits," in *Proc. Solid-State Sensor and Actuator Workshop (Hilton Head '94)*, Hilton Head, SC, June 1994, pp. 251–255.

[5] W. C. Tang, T. C. H. Nguyen, and R. T. Howe, "Laterally driven polysilicon resonant microstructures," *Sensors Actuators*, vol. 20, pp. 25–32, 1989.

[6] H. Fujita and K. J. Gabriel, "New opportunities for microactuators," in *Proc. IEEE Int. Conference on Solid-State Sensors and Actuators (Transducers '91)*, San Francisco, CA, June 1991, pp. 14–20.

[7] T. Akiyama and K. Shono, "Controlled stepwise motion in polysilicon actuators," *J. Microelectromech. Syst.*, vol. 2, no. 3, pp. 106–110, Sept. 1993.

[8] P. Minotti, P. Langlet, G. Bourbon, and T. Masuzawa, "Design and characterization of high-torque/low-speed silicon based electrostatic micromotors using stator/rotor contact interactions," *Japanese J. Appl. Phys.*, vol. 37, no. 3B, pp. L 359–361, March 1998.

[9] P. Langlet, D. Collard, T. Akiyama, and H. Fujita, "A quantitative analysis of scratch drive actuation for integrated X/Y motion system," in *Proc. IEEE Int. Conference on Solid-State Sensors and Actuators (Transducers' 97)*, Chicago, IL, June 1997, pp. 773–776.

[10] T. Ono, D. Y. Sim, and M. Esashi, "Micro-discharge and electric breakdown in a micro-gap," *IOP J. Micromech. Microeng.*, vol. 10, pp. 445–451, 2000.

[11] W. Riethmuller and W. Benecke, "Thermally excited silicon microactuators," *IEEE Trans. Electron Devices*, vol. 35, pp. 758–763, June 1988.

[12] X.-Q. Sun, X. Gu, and W. N. Carr, "Lateral in-plane displacement microactuators with combined thermal and electrostatic drive," in *Proc. Solid-State Sensor and Actuator Workshop*, Hilton Head, SC, June 1996, pp. 152–155.

[13] M. Okyar, X.-Q. Sun, and W. N. Carr, "Thermally excited inchworm actuators and stepwise micromotors: analysis and fabrication," *Proc. SPIE*, vol. 3224, pp. 372–379, 1997.

[14] M. Ataka, A. Omodaka, N. Takeshima, and H. Fujita, "Fabrication and operation of polyimide bimorph actuators for a ciliary motion system," *J. Microelectromech. Syst.*, vol. 2, pp. 146–150, Dec. 1993.

[15] J. W. Suh, R. B. Darling, K.-F. Bohringer, B. R. Donald, H. Baltes, and G. T. A. Kovacs, "CMOS integrated ciliary actuator array as a general-purpose micromanipulation tool for small objects," *J. Microelectromech. Syst.*, vol. 8, no. 4, pp. 483–496, Dec. 1999.

[16] T. Ebefors, J. U. Mattson, E. Kalvesten, and G. Stemme, "A robust micro conveyor realized by arrayed polyimide joint actuators," in *Proc. IEEE Int. Conference on Micro Electro Mechanical Systems (MEMS99)*, Orlando, FL, Jan. 1999.

[17] J. W. Judy, T. Tamagawa, and D. L. Polla, "Surface micromachined linear thermal actuator," *Proc. IEEE Electron Devices Meeting*, pp. 26.5.1–26.5.4, Dec. 1990.

[18] H. Guckel, J. Klein, T. Christenson, K. Skrobis, M. Laudon, and E. G. Lovell, "Thermo-magnetic metal flexure actuators," in *Proc. Solid-State Sensor and Actuator Workshop (Hilton Head '92)*, June 1992, pp. 73–75.

[19] C. G. Keller and R. T. Howe, "Nickel-filled HEXSIL thermally actuated tweezers," in *Proc. IEEE Int. Conference on Solid-State Sensors and Actuators (Transducers' 95)*, Stockholm, Sweden, June 1995, pp. 376–379.

[20] J. H. Comtois, M. A. Michalicek, and C. C. Barron, "Characterization of electrothermal actuators in a four-level, planarized surface-micromachined polycrystalline process," in *Proc. IEEE Int. Conf. on Solid-State Sensors and Actuators (Transducers '97)*, Chicago, IL, June 1997, pp. 769–772.

[21] T. Moulton and G. K. Ananthasuresh, "Micromechanical devices with embedded electro-thermal-compliant actuation," in *Proc. ASME Winter Annu. Meeting*, vol. MEMS-1, 1999, pp. 553–560.

[22] J. Jonsmann, O. Sigmund, and S. Bouwstra, "Compliant electro-thermal microactuators," in *IEEE Conf. on Micro Electro Mechanical Systems*, Orlando, FL, 1999, pp. 588–592.

[23] M. Kohl and K. D. Skrobanek, "Linear microactuators based on shape memory alloy effect," in *Proc. IEEE Int. Conf. on Solid-State Sensors and Actuators (Transducers '97)*, Chicago, IL, June 1997, pp. 785–788.

[24] Y. B. Gianchandani and K. Najafi, "Bent-beam strain sensors," *J. Microelectromech. Syst.*, vol. 5, no. 1, pp. 52–58, Mar. 1996.

[25] N. Takeshima, K. J. Gabriel, M. Ozaki, J. Takahashi, H. Horiguchi, and H. Fujita, "Electrostatic parallelogram actuators," in *Proc. IEEE Int. Conf. on Solid-State Sensors and Actuators (Transducers '91)*, June 1991, pp. 63–66.

[26] L. Que, J.-S. Park, and Y. B. Gianchandani, "Bent-beam electro-thermal actuators for high force applications," in *Proc. IEEE Conf. on Micro Electro Mechanical Systems*, Orlando, FL, Jan. 1999, pp. 31–36.

[27] E. H. Klassen, K. Petersen, J. M. Noworolksi, J. Logan, N. I. Maluf, J. Brown, C. Storment, W. McCulley, and G. T. A. Kovacs, "Silicon fusion bonding and deep reactive ion etching: A new technology for microstructures," in *Proc. Int. Conf. on Solid-State Sensors and Actuators (Transducers '95)*, Stockholm, Sweden, June 1995, pp. 556–559.

[28] J.-S. Park, L. L. Chu, A. D. Oliver, and Y. B. Gianchandani, "Bent-beam electrothermal actuators—Part II: Linear and rotary microengines," *J. Microelectromech. Syst.*, vol. 10, pp. 255–262, June 2001.

[29] W. H. Ko, J. T. Suminto, and G. J. Yeh, "Bonding techniques for microsensors," in *Micromachining and Micropackaging of Sensors*. New York: Elsevier Science, 1985.

[30] Y. B. Gianchandani and K. Najafi, "A bulk silicon dissolved wafer process for microelectromechanical devices," *J. Microelectromech. Syst.*, vol. 1, no. 2, pp. 77–85, June 1992.

[31] Y. B. Gianchandani and K.. Najafi, "Scanning thermal profilers with integrated sensing and actuation," *IEEE Trans. Electron Devices*, vol. 44, no. 11, pp. 1857–68, Nov. 1997.

[32] L. Que, L. Otradovec, A. Oliver, and Y. Gianchandani, "Pulse and dc operation lifetimes of bent-beam electrothermal actuators," in *Proc. IEEE/ASME Int. Conference on Micro Electro Mechanical Systems (MEMS 01)*, Interlaken, Switzerland, Jan. 2001.

Long Que (S'98–M'01) received the B.S. degree in physics and the M.S.E.E. degree in optical communication from Peking University, Beijing, P.R. China, in 1990 and 1994, respectively. He received the M.S. and Ph.D. degree from University of Wisconsin at Madison in 1996 and 2000, respectively, all in electrical engineering.

From 1990 to 1993, he was a Research Engineer at the National Key Lab of Microfabrication on Optical Technology, Institute of Optics and Electronics, Chinese Academy of Sciences, where he focused on the submicron and deep submicron technology research in optical lithography using phase-shifting mask techniques. From 1993 to 1994, he was a Research Assistant in the National Laboratory on Local Fiber-Optic Communication Networks & Advanced Optical Communication Systems, Peking University, where his research was focused on developing optical components in WDM optical communication system. From 1995 to September 2000, he was a Research Assistant at Center for Nanotechnology, ECE Microsystems Lab at University of Wisconsin at Madison, where his research interests included optical imaging formation in systems (MEMS). Since September 2000, he joined as a Research and Development Engineer at OpticNet, Inc., Campbell, CA, where he has been developing optical components using MEMS techniques, such as switch, optical variable attenuator, power splitter, optical coupler, demuxer/muxer, etc., for WDM and DWDM optical communication network. He has been active in microtechnology, nanotechnology and optics for over 10 years. He has published more than a dozen papers in journals and conferences relating to optics, nanothechology, and MEMS area. He has seven patents pending.

Dr. Que received a national research award in the development of submicron and deep submicron IC technology from the Chinese Academy of Sciences in 1997 and also for his work from 1990 to 1993. He received the Vilas development fellowship from University of Wisconsin-Madison in 2000 for his dissertation research work. He is a member of SPIE.

Jae-Sung Park receive the B.S. degree from Pohang University of Science and Technology and the M.S. degree from Seoul National University, Korea, in 1995 and 1997, respectively, both in mechanical engineering. He is currently pursuing the Ph.D. degree in mechanical engineering Department at the University of Wisconsin, Madison.

As a Masters student, he was involved in developing optical probe measurement tools. Since 1997, his research has focused on microelectromechanical systems (MEMS) design and fabrication, with emphasis on microactuators and pressure sensors.

Yogesh B. Gianchandani (S'83–M'95) received the B.S. degree from University of California, Irvine, the M.S. degree from the University of California, Los Angeles, and the Ph.D. degree from the University of Michigan, Ann Arbor, all in electrical engineering, in 1984, 1986, and 1994, respectively.

From 1985 to 1988, he was with Xerox Corporation and from 1988 to 1989, he was with Microchip Technology, Inc., working in the area of integrated circuit design. From 1994 to August 1997, he was a Research Fellow in the Center for Integrated Sensors and Circuits at the University of Michigan, Ann Arbor. Since then he has been with the University of Wisconsin, Madison, as an Assistant Professor in the Department of Electrical and Computer Engineering. His research interests include all aspects of design, fabrication, and packaging of micromachined sensors and actuators and their interface circuits.

Dr. Gianchandani received the National Science Foundation Career Award in 2000. He serves on the editorial boards of two technical journals, and on the steering committee for the IEEE International Conference on Microelectromechanical Systems (MEMS).